Generalized gradient approximation exchange energy functional with correct asymptotic behavior of the corresponding potential

Javier Carmona-Espíndola,[1,a)] José L. Gázquez,[1,2,b)] Alberto Vela,[2] and S. B. Trickey[3]
[1]*Departamento de Química, Universidad Autónoma Metropolitana-Iztapalapa, Av. San Rafael Atlixco 186, México D. F. 09340, México*
[2]*Departamento de Química, Centro de Investigación y de Estudios Avanzados, Av. Instituto Politécnico Nacional 2508, México D. F. 07360, México*
[3]*Quantum Theory Project, Department of Physics and Department of Chemistry, University of Florida, P.O. Box 118435, Gainesville, Florida 32611-8435, USA*

(Received 12 June 2014; accepted 13 January 2015; published online 4 February 2015)

A new non-empirical exchange energy functional of the generalized gradient approximation (GGA) type, which gives an exchange potential with the correct asymptotic behavior, is developed and explored. In combination with the Perdew-Burke-Ernzerhof (PBE) correlation energy functional, the new CAP-PBE (CAP stands for correct asymptotic potential) exchange-correlation functional gives heats of formation, ionization potentials, electron affinities, proton affinities, binding energies of weakly interacting systems, barrier heights for hydrogen and non-hydrogen transfer reactions, bond distances, and harmonic frequencies on standard test sets that are fully competitive with those obtained from other GGA-type functionals that do not have the correct asymptotic exchange potential behavior. Distinct from them, the new functional provides important improvements in quantities dependent upon response functions, e.g., static and dynamic polarizabilities and hyperpolarizabilities. CAP combined with the Lee-Yang-Parr correlation functional gives roughly equivalent results. Consideration of the computed dynamical polarizabilities in the context of the broad spectrum of other properties considered tips the balance to the non-empirical CAP-PBE combination. Intriguingly, these improvements arise primarily from improvements in the highest occupied and lowest unoccupied molecular orbitals, and not from shifts in the associated eigenvalues. Those eigenvalues do not change dramatically with respect to eigenvalues from other GGA-type functionals that do not provide the correct asymptotic behavior of the potential. Unexpected behavior of the potential at intermediate distances from the nucleus explains this unexpected result and indicates a clear route for improvement. © *2015 AIP Publishing LLC.* [http://dx.doi.org/10.1063/1.4906606]

I. INTRODUCTION

Density functional methods[1] in the Kohn-Sham (KS) formulation[2] have become the most common approach to electronic structure calculations of atoms, molecules, and solids.[3–11] Though present-day approximations to the exchange-correlation (XC) energy functional enable calculations with rather reasonable computational effort even on large systems, the need continues for better balanced descriptions of thermodynamic, structural, and response properties at each rung of the Jacobs' ladder[12] above the local density approximation (LDA). Improved generalized gradient approximations (GGAs) are particularly desirable,[13–16] both because of the wide range of accessible systems at near-minimal computational cost (since GGAs have no explicit orbital dependence) and because a GGA usually is a foundational component of higher-rung functionals. A GGA exchange (X) functional in general can be expressed as

$$E_x^{GGA}[\rho] = \int \rho(\mathbf{r}) e_x^{LDA}[\rho;\mathbf{r}] F_x(s) d\mathbf{r} = \int e_x[\rho,s;\mathbf{r}] d\mathbf{r}, \quad (1)$$

where

$$e_x^{LDA}[\rho;\mathbf{r}] = A_x \rho(\mathbf{r})^{1/3}, \quad \text{with} \quad A_x = -\frac{3(3\pi^2)^{1/3}}{4\pi}, \quad (2)$$

and

$$s(\mathbf{r}) = \frac{1}{2k_F(\mathbf{r})} \frac{|\nabla\rho(\mathbf{r})|}{\rho(\mathbf{r})}, \quad \text{with} \quad k_F(\mathbf{r}) = (3\pi^2\rho(\mathbf{r}))^{1/3}. \quad (3)$$

The enhancement factor $F_x(s)$ describes deviations from local homogeneous electron gas (HEG) behavior. Typically, it is expressed as an analytical function of s that depends on several parameters. Empirical procedures set at least some parameters by minimizing the mean absolute error (MAE) in the calculated values of several properties relative to well-known test sets.[17–27] Non-empirical procedures fix the parameters by imposition of conditions known to be obeyed by the exact XC energy functional.

The analytical forms of most current GGA X functionals are designed to satisfy constraints related to the properties of E_x (and, sometimes, the canonical exchange-energy density) at small and large s-values. At small s, one has

$$F_x(s) \xrightarrow[s\to 0]{} 1 + \mu s^2 + \cdots, \quad (4)$$

[a)]E-mail: jcarmona_26@yahoo.com.mx
[b)]E-mail: jlgm@xanum.uam.mx

where μ may be fixed in various non-empirical ways. That diversity is an example of design choices that occur in constraint-based functional development. The gradient expansion approximation (GEA) yields[28] $\mu_{GEA} = 10/81 \approx 0.1235$. In the Perdew-Burke-Ernzerhof (PBE) functional,[15] μ is fixed to cancel the second-order gradient contribution to the correlation energy in the high density limit,[15] so as to recover the LDA linear response behavior, which is known to be rather good. With the Ma and Brueckner[29] correlation energy result, one finds $\mu_{PBE} = 0.2195$. Alternatively, the asymptotic expansion of the semi-classical neutral atom yields a modified gradient expansion approximation[30] with $\mu_{MGEA} = 0.26$. One also can fix μ so that the X energy for the exact ground state density of the hydrogen atom cancels the spurious electron-electron Coulomb repulsion for that density, thereby obtaining an X functional which is approximately one-electron self-interaction free.[31] The resulting μ value depends on the particular analytical form chosen for $F_x(s)$, together with the values of the other parameters present in it.

The enhancement factor behavior at large s also depends on the constraint used. For example, to guarantee satisfaction of the Lieb-Oxford (L-O) bound[32,33] for all densities, that bound is imposed locally in PBE X, that is, on the integrand of the RHS of Eq. (1). Thus, $F_x^{PBE}(s)$ grows monotonically from unity at $s = 0$ (to recover the HEG, as must all non-empirical functionals) to a limiting value of 1.804 as $s \to \infty$. In the VMT X functional,[34] $F_x^{VMT}(s)$ also grows to a maximum determined by the local Lieb-Oxford bound, but then decreases back to unity as $s \to \infty$, so as to recover the HEG limit. The $F_x(s)$ factors for the PW91,[35] VT84,[36] and PBE-LS[37] functionals, all go to a local Lieb-Oxford bound maximum, and then, as $s \to \infty$, decrease to zero faster than $s^{-1/2}$ to fulfill the non-uniform density scaling result.[33] Exact satisfaction of that constraint would imply[38–41] that the enhancement function should decrease to zero proportionally to $s^{-1/2}$. An empirical functional that also decreases to zero faster than $s^{-1/2}$ was proposed by Lacks and Gordon,[42] but its maximum is unrelated to the local Lieb-Oxford bound.

Arguing from a different perspective, there have been other approximations, e.g., such as the B88 functional,[13] in which $F_x(s)$ is designed to reproduce the asymptotic behavior of the conventional (i.e., canonical) exact exchange energy density

$$e_x[\rho,s;\mathbf{r}] \xrightarrow[r\to\infty]{} -\frac{\rho(\mathbf{r})}{2r}, \tag{5}$$

which for a GGA is equivalent to[43]

$$F_x(s) \xrightarrow[s\to\infty]{} a\, s/\ln s, \tag{6}$$

where a is a constant. Despite this divergence in $F_x(s)$ as $s \to \infty$, the whole integrand of the first equality in Eq. (1) tends to zero when $r \to \infty$, so that the exchange energy is finite. Another enhancement factor that also diverges for large s, but as $s^{2/5}$, is PW86,[44] which follows from the gradient expansion of the exchange hole with real space cutoffs. The relevance of this large s limit has been analyzed by Murray, Lee, and Langreth.[45]

Broadly speaking, all these $F_x(s)$ forms provide a reasonable description of properties that depend on total energy differences, although there are important and subtle differences among them. However, for finite systems, those approximate forms of $F_x(s)$ give KS eigenvalues and orbitals which have undesirable consequences for the calculation of response properties such as the static and dynamic polarizabilities and hyperpolarizabilities. In particular, it long has been known that the asymptotic behavior of the XC potential plays a fundamental role in the description of excitation energies determined from time dependent density functional theory (TDDFT).[46,47] Additionally, recently, there has been discussion to the effect that accurate XC potentials are essential for getting accurate energies.[48] Thus, it seems worthwhile to incorporate constraints specific to the X potential, because of its direct connection to the KS eigenvalues and orbitals.

The X potential,

$$v_x[\rho;\mathbf{r}] = \frac{\delta E_x[\rho]}{\delta \rho(\mathbf{r})}, \tag{7}$$

has two important properties which are related to the KS eigenvalues and orbitals, namely, its discontinuity with respect to particle number N[49–52] and its asymptotic behavior.[53–55] No simple N-independent GGA can mimic, by itself, the linear dependence of E_{tot} on N that underlies the derivative discontinuity (though there are prescriptions for adding such behavior[56–60]), so we put the issue aside. The asymptotic behavior of the X potential is

$$v_x[\rho;\mathbf{r}] \xrightarrow[r\to\infty]{} -\frac{1}{r}. \tag{8}$$

Most current GGA-type X functionals, e.g., PBE, VMT, VT84, PBE-LS, and many others, yield v_x that decays exponentially. Although the B88 X functional fulfills Eq. (5), its functional derivative decays as $-h/r^2$ (h is a constant related to the asymptotic behavior of ρ), because all the terms with $-1/r$ behavior cancel. Since violation of Eq. (8) causes problems for response properties dependent upon the KS eigenvalues and on the orbital behavior in distant regions, there have been several attempts at direct construction of a GGA X potential with the correct asymptotic behavior,[43,61–63] Eq. (8). Such potentials certainly improve the description of response properties. But their utility is severely limited by the fact that they are not the functional derivative of an X energy functional, Eq. (7). The total energy obtained via such a potential, therefore, is not a variational extremum, and associated total energy differences are of questionable validity. Additionally, recently, it has been shown[64] that the description of electronic excitations also is severely limited when using XC potentials that are not the functional derivative of an XC energy functional.

While there are higher-rung X functionals that yield an X potential with the correct asymptotic behavior, those add dependence upon the Laplacian of the density[65–67] at minimum. That adds computational complexity, hence cost. Similarly, incorporation of correct asymptotic behavior through non-local procedures[68–72] introduces a substantial increase in computational effort. Thus, it seems worthwhile to attempt incorporation of correct asymptotic behavior in a non-empirical GGA X functional. Here, we present such a functional and show that it retains the quality of calculated thermodynamic and kinetic properties associated with current

GGA functionals while improving the description of response properties.

After summarizing the formal development, we report validation of the new X functional via the customary calculations on diverse data sets. We compare with results from several current GGA functionals in the prediction of properties that depend on energy differences. Then, we report results for the new X functional for static and dynamic polarizabilities and hyperpolarizabilities and assess the results.

II. CORRECT ASYMPTOTIC POTENTIAL ("CAP") GGA EXCHANGE ENERGY FUNCTIONAL

The general expression for the GGA X potential in terms of the X energy density from the first equality of Eq. (1) is

$$\begin{aligned} v_x^{GGA}[\rho;\mathbf{r}] = {} & A_x\rho(\mathbf{r})^{1/3}\left[\frac{4}{3}F_x(s)\right] \\ & + A_x\rho(\mathbf{r})^{1/3}\left[-\frac{4}{3}s(\mathbf{r}) - \frac{1}{2k_F}\frac{\nabla^2\rho(\mathbf{r})}{|\nabla\rho(\mathbf{r})|}\right. \\ & \left. + \frac{1}{2k_F}\frac{\nabla\rho(\mathbf{r})\cdot\nabla|\nabla\rho(\mathbf{r})|}{|\nabla\rho(\mathbf{r})|^2}\right]\frac{dF_x(s)}{ds} \\ & + A_x\rho(\mathbf{r})^{1/3}\left[-\frac{1}{(2k_F)^2}\frac{\nabla\rho(\mathbf{r})\cdot\nabla|\nabla\rho(\mathbf{r})|}{|\nabla\rho(\mathbf{r})|\rho(\mathbf{r})}\right. \\ & \left. + \frac{4}{3}s(\mathbf{r})^2\right]\frac{d^2F_x(s)}{ds^2}. \end{aligned} \tag{9}$$

Observe that the gradient terms in the denominators cancel if the enhancement function behaves as in Eq. (4) as $s \to 0$. This fact underscores the relevance of using GGA enhancement functions that fulfill the limit given by Eq. (4).

Correct asymptotic behavior of the X potential depends upon the asymptotic behavior of the density, namely,[73–75]

$$\rho(r) \xrightarrow[r\to\infty]{} \rho_0 r^{\alpha} e^{-\lambda r}. \tag{10}$$

From this, Eq. (9) becomes

$$\begin{aligned} v_x^{GGA}[\rho;\mathbf{r}] \xrightarrow[r\to\infty]{} {} & A_x\rho(r)^{1/3}\left[\frac{4}{3}\right]F_x \\ & + A_x\rho(r)^{1/3}\left[-\frac{4}{3}s(r) + \frac{2}{\lambda r}s(r)\right]\frac{dF_x}{ds} \\ & + A_x\rho(r)^{1/3}\left[\frac{1}{3}s(r)^2\right]\frac{d^2F_x}{ds^2}. \end{aligned} \tag{11}$$

An equivalent expression was derived by Engel and collaborators,[76] who showed that if the enhancement factor behaves as

$$F_x(s) \xrightarrow[s\to\infty]{} -\frac{(3\pi^2)^{1/3}}{A_x}s, \tag{12}$$

then, since the reduced density gradient in that limit goes as

$$s(r) \xrightarrow[r\to\infty]{} \frac{1}{2(3\pi^2\rho(r))^{1/3}}\,\lambda\left(1-\frac{\alpha}{\lambda r}\right), \tag{13}$$

one finds [substitute Eqs. (12) and (13) in (11)] that the leading term in the X potential decays correctly, e.g., per Eq. (8).

The asymptotic behaviors of $F_x(s)$ in Eqs. (12) and (6) obviously are incompatible, which follows from the equally obvious fact that a GGA functional cannot satisfy both Eqs. (8) and (5). Note also that (12) is incompatible with the uniform scaling asymptotics[33] proportional to $s^{-1/2}$. However, Eq. (8) appears to be important for response functions whereas calculations show that the values of the enhancement function when $s \to \infty$ only weakly influence the X energy[37] [because this region corresponds to very small ρ]. Our experience with the uniform scaling asymptotics[34,36,37] shows that they do not strongly affect the results either (except indirectly as they influence the small-s behavior because of a specific functional form for F_x). Therefore, we enforce Eq. (8) instead of those other constraints. This is a design choice which differs from our previous ones[34,36,37] because of different motivations. The key to such choices is to resolve which ones yield the most broadly useful X functional, with clear insight into the cause. One may be concerned that enforcement of Eq. (8) leaves open the certainty of violation of the Lieb-Oxford bound for some arbitrary density. However, were such a density to be found, it seems plausible that it would be remote from the neighborhood of ground-state densities, and the practical consequences of such a violation would be negligible compared to the utilitarian simplicity of a GGA X functional. In the numerical studies presented below, this speculation is confirmed. We find no example of violation of the L-O bound by the new functional we present next.[77] In contrast, the gedanken density recently proposed by Perdew and collaborators,[41] which is far from the densities for real systems, was built so that any enhancement function that takes values above 1.804 violates the global Lieb-Oxford bound. Thus, enhancement functions that diverge when $s \to \infty$, such as those that fulfill Eq. (6) or (12), violate the Lieb-Oxford bound for this gedanken density, as is shown in detail in the supplementary material.[77] Our results (as well as those with the B88 X functional) suggest that one may be reasonably confident that such violations occur only in extreme situations.

To proceed, we need a form of $F_x(s)$ that reduces to Eq. (4) as $s \to 0$ and to Eq. (12) as $s \to \infty$. Additionally, it seems prudent to select a form which is close to good current GGA functionals on $0 \le s \le 3$, a region known to be important for the total energy.[78–80] Thus, we propose

$$F_x^{CAP}(s) = 1 - \frac{\alpha}{A_x}\frac{s\ln(1+s)}{1+c\ln(1+s)}. \tag{14}$$

The superscript stands for "correct asymptotic potential." Observe that a $\ln(1+s)$ dependence in F_x has been discussed recently.[81] The constant c is fixed to fulfill Eq. (12), $c = \alpha/(3\pi^2)^{1/3}$, and α is fixed from Eq. (4), leading to $\alpha = -A_x\mu$. As mentioned, μ may be fixed via several non-empirical procedures, so one can test Eq. (14) with those different values, another design choice. For convenience of computational implementation, the ingredients of v_x^{CAP} are given in the Appendix. We return to its detailed form below.

Fig. 1 shows the new X enhancement factor (Eq. (14)), on $0 \le s \le 3$, for $\alpha = -A_x\mu$ fixed via $\mu_{PBE} = 0.2195$. Fig. 1 also shows the B88,[13] PBE,[15] PBE-LS,[37] and OPTX[16] enhancement factors. Observe that F_x^{CAP} lies below all the others for s between 0 and about 1.7, after which they all separate. The B88 form, as noted, was constructed to satisfy Eq. (5), leading to the divergence of the form given by Eq. (6). Recall also the discussion above about large-s behaviors and satisfaction

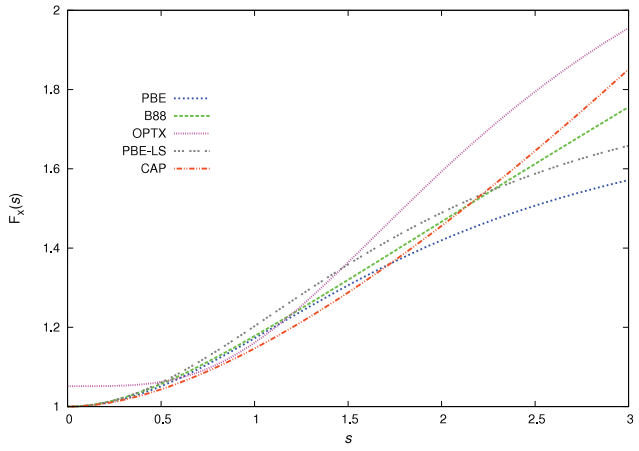

FIG. 1. Comparison of several enhancement functions in the interval $0 \le s \le 3$.

of the local Lieb-Oxford bound for various functionals. Also note that the empirical parameters in the OPTX functional are fixed to obtain the minimum error in the total Hartree-Fock energy of the first eighteen atoms of the periodic table.

III. RESULTS AND DISCUSSION

With the objective of improving response properties without sacrificing the quality of thermodynamic, structural, and kinetic properties obtained with current GGA functionals, we first considered the consequences of different non-empirical μ values (recall discussion in Sec. I) and associated $\alpha = -A_x\,\mu$ values to determine which μ gives the best description of properties that depend on energy differences. Thus, we did calculations of heats of formation using the G3/99 test set[17] (data for 223 molecules) with the α values corresponding to the different non-empirical μ values summarized in Sec. I. We used both the PBE[15] or Lee-Yang-Parr (LYP)[14] correlation energy functionals. The calculations used a developmental version of the program NWChem6.0.[82] The protocol for calculating heats of formation was as established in Ref. 83 and described previously.[31] MAE results for the Def2-TZVPP basis set[84] for the different combinations are presented in Table I. One sees that the lowest MAE is obtained for α from $\mu_{PBE} = 0.2195$, in combination with the PBE C functional. Next best is CAP X with LYP C for the same μ. Thus, all subsequent calculations presented in this work were done with $F_x^{CAP}(s)$ from Eq. (14), with $\alpha = -A_x\,\mu$ and $\mu_{PBE} = 0.2195$. Recall that the PBE C functional used in Table I corresponds to the Ma and Brueckner,[15,29] value $\beta = 0.066\,725$ through the relationship $\mu = \pi^2\beta/3$. It has become a common practice to use that relationship between μ and β to fix the value of the latter when μ different from $\mu_{PBE} = 0.2195$ is considered.[31,85] We tried that with the PBE C functional and found MAEs of 65.88 kcal/mol, 28.29 kcal/mol, and 31.21 kcal/mol for $\mu_{GEA} = 10/81 \approx 0.1235$, $\mu_{MGEA} = 0.26$, and $\mu_{SICH} = 0.2646$, respectively. All those errors are worse than for the $\beta = 0.066\,725$ of the original PBE C energy.

Comparison calculations used the LDA,[86,87] PBE,[15] BLYP (B88 X with LYP C),[13,14] PBE-LS,[37] and OLYP (Optimized X with LYP C)[14,16] X functionals. All calculations were done with the same developmental version of NWChem6.0 and the same protocol for the heats of formation. Ionization potentials and electron affinities were obtained for the IP13/3[19] (6 molecules) and EA13/3[25] (7 molecules) datasets, respectively. The molecular calculations were done adiabatically according to the geometries reported in Ref. 88. Proton affinities were calculated for the PA8[18,26] dataset (8 molecules). For the geometries of the anions and neutral species, MP2(full)/6-31G (2df,p) calculations were used.[89] Binding energies of weakly interacting systems were calculated for the HB6/04,[21] CT7/04,[21] DI6/04,[21] WI7/05,[22] and PPS5/05[22] datasets (31 systems). Ionization potentials, electron affinities, proton affinities, and binding energies were calculated with the 6-31++G(d,p) basis set. Barrier heights for forward and backward transition states of 19 hydrogen and 19 non-hydrogen transfer reactions were done for the HTBH38/04[22–24,27] and the NHTBH38/04[22–24,27] datasets, respectively. Bond distance calculations were done for the T-96R[20] dataset (96 molecules). Experimental bond distances for this analysis were taken from Ref. 90. Finally, harmonic frequencies were calculated for the T-82F[20] dataset (82 molecules), with experimental values from Refs. 90–92. Barrier heights, bond distances, and vibrational frequencies were calculated with the Def2-TZVPP basis set.

TABLE I. Comparison of mean absolute errors in kcal/mol for the heats of formation for the G3 test set (223 molecules) with the X energy functional given by Eqs. (1) and (14) for different values of μ with either the LYP[a] or PBE[b] C energy functional.

μ	E_{xc}	MAE
10/81[c]	CAP-LYP	49.58
10/81[c]	CAP-PBE	59.49
0.2195[d]	CAP-LYP	12.41
0.2195[d]	CAP-PBE	9.23
0.26[e]	CAP-LYP	33.03
0.26[e]	CAP-PBE	24.70
0.2646[f]	CAP-LYP	35.54
0.2646[f]	CAP-PBE	27.18

[a]Reference 14.
[b]Reference 15.
[c]Gradient expansion approximation value.
[d]PBE value.
[e]Modified gradient expansion approximation value.
[f]Self-interaction correction for the hydrogen atom with the exchange functional given by Eqs. (1) and (14).

Table II shows the MAE results for those various property comparisons. Individual deviations for each property are given in the supplementary material.[77] Clearly, CAP-PBE (i.e., CAP X with PBE correlation C) provides a rather good description of all those properties and is fully competitive with PBE-LS. Except for the heats of formation, it is fully competitive with OLYP, which is known to be among the better empirical GGA functionals for thermodynamic, kinetic, and structural properties. More significant, from the perspective of design choice, is the fact that the CAP-PBE, PBE-LS, and OLYP enhancement factor functional forms are so qualitatively different. The difference is particularly striking in the case of PBE-LS and CAP-PBE, which share the same C functional. Their MAE outcomes are, in general, close to each other,

TABLE II. MAEs for the different exchange-correlation functionals, for several properties. Energies in kcal/mol, bond distances in Å, and frequencies in cm^{-1}.

Property	LDA	PBE	BLYP	OLYP	PBE-LS	CAP-LYP	CAP-PBE
Heats of formation	118.32	21.21	9.64	5.51	9.39	12.41	9.23
Ionization potentials	5.31	3.47	4.20	2.61	3.65	4.62	2.55
Electron affinities	6.62	2.64	2.97	3.63	2.61	3.84	3.65
Proton affinities	5.65	1.39	1.78	1.66	1.23	1.41	1.53
Binding energies of weakly interacting systems	3.61	1.64	1.67	2.27	1.49	2.41	2.70
Reaction barrier heights							
Hydrogen transfer forward	18.41	9.49	7.81	6.02	7.26	7.09	6.92
Hydrogen transfer backward	17.16	9.72	7.85	6.06	7.77	7.06	7.11
Non-hydrogen transfer forward	14.02	10.38	10.48	7.74	9.45	9.45	8.22
Non-hydrogen transfer backward	12.51	9.96	10.03	7.21	9.31	9.06	7.99
Bond distances	0.0149	0.0179	0.0240	0.0198	0.0216	0.0255	0.0221
Frequencies	50.89	43.30	56.25	40.42	45.74	58.42	46.15

despite opposite behaviors in the large s limit (PBE-LS goes to zero exponentially while CAP diverges) and distinctly different behaviors relative to PBE on $0 \le s \le 3$; recall Fig. 1. The combination of CAP X with LYP C leads to a somewhat similar description, though generally not as good as the combination with PBE C. This is especially the case for heats of formation and forward and backward barrier heights of non-hydrogen transfer reactions. As an additional test of F_x^{CAP}, we performed X-only calculations for the noble gas atoms to compare E_x^{CAP} values with those from LDA, PBE, B88, PBE-LS, and OPTX, all referenced to the Hartree-Fock values. The calculations were done using the universal gaussian basis set[93] (UGBS) and the same developmental version of NWChem6.0. See Table III. Unsurprisingly, B88, which was designed to reproduce HF X energies, is best on this test. PBE-LS, which is approximately one-electron self-interaction free, is next best. CAP is better than OPTX but has more than twice the MAE of PBE. These outcomes illustrate the general difficulty of designing GGA XC functionals. Improvement on one figure of merit often leads to loss of accuracy on another. Here, the emphasis on the accuracy of the X potential has caused a loss of accuracy in the X energy when compared to the atomic Hartree-Fock values.

For response properties, we calculated static and dynamic polarizabilities and hyperpolarizabilities via TDDFT as implemented recently in time-dependent auxiliary density perturbation theory (TDADPT) form[94–98] in the code deMon2k, pre-release version 4.2.2.[99,100] We used the TZVP-FIP1 basis sets.[101,102] TDADPT uses the expansion of the density as a linear combination of Hermite Gaussian functions[103,104] called the auxiliary density in deMon2k. We used the GEN-A2* auxiliary function set[105] for that expansion in all the response calculations. As a technical matter, we followed the familiar procedure[58,106–108] of evaluating the TDDFT kernel $f_{xc} = \delta v_{xc}/\delta\rho$ and kernel derivative, $g_{xc} = \delta f_{xc}/\delta\rho = \delta^2 v_{xc}/\delta\rho^2$ in the adiabatic local density approximation (ALDA). That is, the LDA functional derivatives were used rather than the CAP or other GGA derivatives. The original rationale for that approximation was (and is) that the GGA derivatives have complicated internal structure that tends to cause serious numerical instabilities. These problems could be addressed in the future through the use of analytical rather than numerical derivatives but at present they are a limitation. It is critical to note, however, that the previous efforts to mend or repair the incorrect asymptotic potential in TDDFT, which we discussed at the outset, *also* used the ALDA derivatives as well. Thus, our first principles v_x^{CAP} first must be tested in the *same* context. To minimize numerical noise, the XC energy, potential, TDDFT kernel, and kernel derivative were integrated numerically on the so-called reference grid[109] in deMon2k. The mean polarizabilities were calculated from the diagonal elements of the polarizability tensor according to

$$\bar{\alpha}(\omega) = \frac{1}{3}\left(\alpha_{xx}(\omega) + \alpha_{yy}(\omega) + \alpha_{zz}(\omega)\right). \tag{15}$$

For the calculation of hyperpolarizabilities, we employed the so-called EFISH (electric-field-induced second-harmonic) orientation. The average hyperpolarizability was calculated

TABLE III. Exchange energies and MAEs with respect to Hartree-Fock values of noble gas atoms, in hartree, as determined by exchange-only calculations with the universal gaussian basis set[a] for several exchange energy functionals.

Atom	LDA	PBE	B88	OPTX	PBE-LS	CAP	HF
He	−0.852 78	−1.001 65	−1.016 05	−1.018 77	−1.028 10	−0.9972 3	−1.025 77
Ne	−10.937 08	−12.008 39	−12.086 29	−12.087 55	−12.200 95	−11.872 74	−12.108 35
Ar	−27.774 98	−29.956 17	−30.122 03	−30.188 95	−30.350 03	−29.644 45	−30.184 99
Kr	−88.479 27	−93.338 60	−93.798 97	−94.652 47	−94.221 65	−92.620 09	−93.856 05
Xe	−170.447 13	−178.191 29	−179.004 86	−181.419 49	−179.602 77	−177.057 44	−179.097 57
Rn	−372.802 15	−385.831 67	−387.402 36	−395.043 19	−388.211 75	−383.996 27	−387.503 81
MAE	5.414	0.575	0.058	1.782	0.306	1.265	

[a]Reference 93.

TABLE IV. Comparison of static LDA and GGA TDADPT hyperpolarizabilities (in a.u.) with TDHF and CCSD(T) values from Ref. 114.

Molecule	LDA	PBE	BLYP	OLYP	PBE-LS	CAP-LYP	CAP-PBE	TDHF	CCSD(T)
H_2O	−21.88	−22.18	−23.89	−24.55	−22.03	−19.86	−16.29	−10.80	−18.00
NH_3	−30.03	−30.11	−32.06	−32.29	−31.32	−33.83	−31.68	−15.20	−34.30
CO	23.44	22.24	24.13	21.09	21.42	22.04	21.51	21.20	23.50
HF	−9.63	−10.04	−10.91	−12.00	−10.47	−11.16	−9.02	−5.38	−7.20
H_2S	−4.71	−5.08	−4.34	−5.90	−5.95	−9.87	−8.38	2.20	−7.70

from

$$\bar{\beta}(-\omega_3;\omega_1,\omega_2) = \frac{1}{5}\sum_i (\beta_{zii} + \beta_{izi} + \beta_{iiz}), \qquad (16)$$

where i runs over x, y, and z. In all response calculations, experimental molecular structures were employed.[110–113]

Table IV shows calculated static hyperpolarizabilities of five small molecules, including both CCSD(T) and time dependent Hartee-Fock (TDHF) calculations.[114] Although TDHF values often exhibit large deviations from CCSD(T) results, they are presented for completeness. The overall trend from the table is that either CAP-PBE or CAP-LYP is preferable, but a decisive choice between the two cannot be made from those data alone. In H_2O, the CAP-PBE hyperpolarizability is rather close to the CCSD(T) value, while all other functionals give similar overestimates in absolute value relative to the CCSD(T) result. For NH_3, the CAP-LYP, BLYP, and OLYP results lie very close to the CCSD(T) value, while the LDA, PBE, PBE-LS, and CAP-PBE values are underestimates (in magnitude). For CO, all functionals perform similarly, with a modest advantage to BLYP, CAP-LYP, and LDA. For HF, the CAP-PBE hyperpolarizability is notably closer to the CCSD(T) value, while all other functionals overestimate the absolute value substantially. In H_2S, both the CAP-PBE and CAP-LYP values are close to that from CCSD(T), while all the other functionals give less negative values.

Table V presents static hyperpolarizabilities of methane analogs with comparisons to available theoretical results. One sees that for CH_3OH, LDA, PBE, PBE-LS, BLYP, and OLYP static hyperpolarizabilities severely overestimate (absolute values) the published CCSD value[115] by at least 14 a.u. In contrast, CAP-LYP reduces the error substantially, and CAP-PBE essentially eliminates the error. In CH_3F, the signs of our hyperpolarizability results, using EFISH orientation, differ from the published LDA result but not the published HF one.[116] Comparison of absolute values shows that our LDA, PBE, BLYP, and OLYP hyperpolarizabilities agree well with the LDA result from Ref. 116. Both the CAP-PBE and CAP-LYP values differ from all the rest, with CAP-PBE and Hartree-Fock results[116] being relatively close in value and with the same sign. For CH_3CN, CAP-PBE clearly is superior to all the other functionals relative to the CCSD(T) value, 116, whereas PBE, PBE-LS, and CAP-LYP values all are rather similar to the LDA result.[116] For the remaining systems reported in Table V, reliable theoretical or experimental values are not available and the one Hartree-Fock value[117] does not seem reasonable in context. Overall, Table V suggests a preference to CAP-PBE.

We proceed to the dynamic mean polarizabilities. Figs. 2–5 present results for H_2O, NH_3, CH_4, and benzene, respectively, including experimental values. In all cases, the experimental frequency ranges are considered. For comparison of the theoretical and experimental values, it is important to bear thermal effects in mind. They are not included in the theoretical values. It is known that thermal effects shift the theoretical values upward (by about 1 a.u.),[118] a key interpretive fact in assessing the dynamic mean polarizability results.

For H_2O, Fig. 2 shows that the LDA, PBE, BLYP, OLYP, and PBE-LS functionals all overestimate the polarizability, with a frequency dependence which is too strong, even over the relatively small experimental range. Observe that the CAP-LYP values *without* thermal correction agree with experimental values. Thermal correction will move the CAP-LYP values above experiment but move the CAP-PBE values closer to experiment. For NH_3 (Fig. 3) and CH_4 (Fig. 4), the only two

TABLE V. Comparison of static LDA and GGA TDADPT hyperpolarizabilities (in a.u.) of methane analogs with other theoretical results.

Molecule	LDA	PBE	BLYP	OLYP	PBE-LS	CAP-LYP	CAP-PBE	Other theoretical results
CH_3OH	−47.31	−47.44	−51.22	−54.30	−48.69	−43.13	−35.79	−33.52[a]
CH_3F	−58.84	−58.34	−62.75	−66.19	−57.48	−46.54	−39.54	36.23[b]; 62.22[c]
CH_3CN	23.55	23.17	22.79	22.48	21.10	27.49	24.50	4.09[b]; 22.76[c]; 24.24[d]
CH_3Cl	−2.98	−2.75	−5.46	−9.73	−1.10	−3.45	6.63	
CHF_3	−31.74	−31.38	−33.00	−33.69	−31.23	−29.23	−28.69	−19.04[e]
CF_3Cl	−72.73	−73.37	−76.86	−75.20	−70.66	−63.61	−60.95	
$CHCl_3$	−2.64	−3.20	−0.42	−5.29	−4.69	−12.21	−3.91	
$CFCl_3$	−34.41	−34.61	−35.60	−32.47	−31.88	−30.73	−27.54	

[a]CCSD from Ref. 115.
[b]Hartree-Fock from Ref. 116.
[c]LDA from Ref. 116.
[d]CCSD(T) from Ref. 116.
[e]Hartree-Fock from Ref. 117.

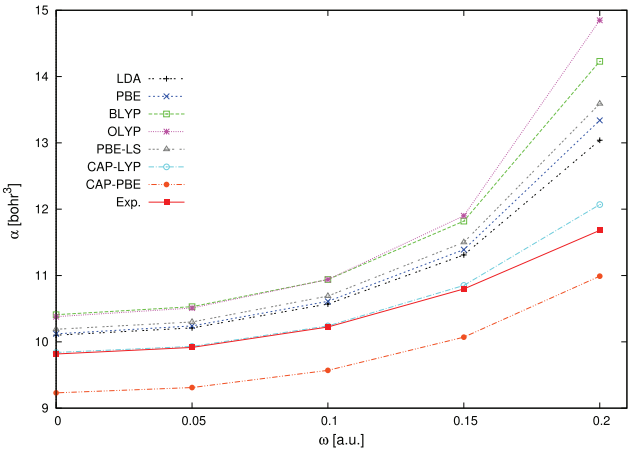

FIG. 2. Static and dynamic polarizabilities of H_2O as a function of ω, calculated with the experimental geometry.

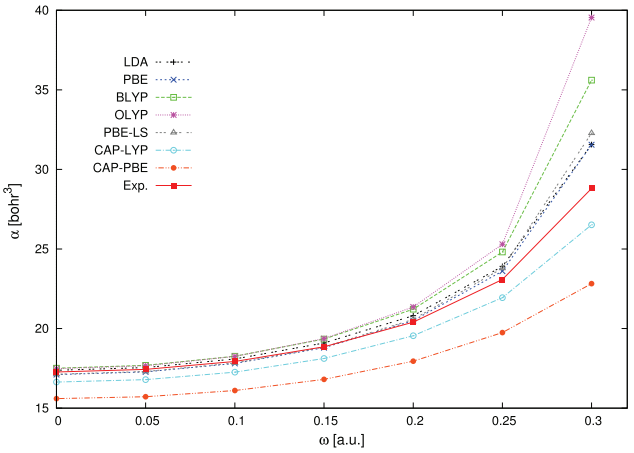

FIG. 4. Static and dynamic polarizabilities of CH_4 as a function of ω, calculated with the experimental geometry.

functionals that give qualitatively correct frequency dependence are CAP-PBE and CAP-LYP. Thus, thermally corrected CAP-PBE and CAP-LYP are expected to give a rather satisfactory description.

For benzene[119] (Fig. 5), the frequency dependence generated by all the functionals is essentially identical and close to that from experiment. However, all of the other functionals, LDA, PBE, PBE-LS, BLYP, and OLYP, overestimate the experimental polarizabilities at least by 3 a.u. before thermal correction, which will worsen the error. The uncorrected CAP-LYP values lie almost atop experiment but after correction will lie above, while CAP-PBE values will lie below or near the experimental results.

Table VI compares dynamic hyperpolarizabilities of the same five small molecules as in Table IV with respect to values from CCSD(T) calculations and from experiment. All the calculations are for the experimental wavelength, 694.3 nm. For H_2O, the CAP-PBE functional gives values of second-harmonic generation (SHG) and OR (optical rectification) hyperpolarizabilities that lie very close to the CCSD(T) results, while all other functionals overestimate both in absolute value. In NH_3, LDA, PBE, PBE-LS, BLYP, OLYP, and CAP-LYP tend to overestimate the SHG absolute value relative to both CCSD(T) and to experiment, whereas CAP-PBE lies rather close to the experimental value. The OR absolute values from all functionals match well with CCSD(T). For CO, LDA, PBE, BLYP, and CAP-LYP give SHG and OR hyperpolarizabilities in good agreement with the reference values, but OLYP, PBE-LS, and CAP-PBE modestly underestimate them. In the HF molecule, LDA, PBE, and CAP-PBE results agree well with the SHG and OR references, whereas BLYP, OLYP, and CAP-LYP tend to somewhat larger overestimated absolute values. For H_2S, all functionals give good results. Again, one can see that overall CAP-PBE is consistently closer to CCSD(T) and experimental results.

Table VII shows dynamic hyperpolarizabilities for the same methane analogs as were considered in Table V. All LDA and GGA functional calculations for SHG were done at the same wavelength as the corresponding experiments. In CH_3OH, the SHG result for CAP-PBE is in good agreement with respect to the CCSD[115] and relatively close to the experimental value,[120] whereas all the other functionals overestimate the absolute values. Note that this overestimation

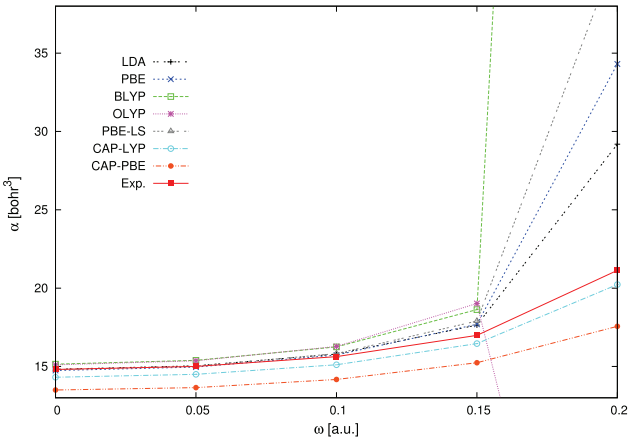

FIG. 3. Static and dynamic polarizabilities of NH_3 as a function of ω, calculated with the experimental geometry.

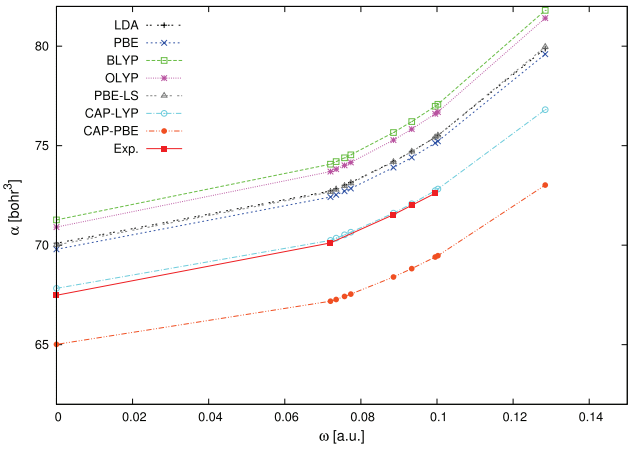

FIG. 5. Comparison of LDA and GGA dynamic polarizabilities with the experimental values for benzene. The experimental geometry was used in all calculations.

TABLE VI. Comparison of dynamic LDA and GGA TDADPT hyperpolarizabilities (in a.u.) with TDHF, CCSD(T), and experimental values for a wavelength of 694.3 nm.

Molecule	Value	LDA	PBE	BLYP	OLYP	PBE-LS	CAP-LYP	CAP-PBE	TDHF[a]	CCSD(T)[a]	Expt.
H_2O	SHG	−28.38	−28.84	−31.57	−32.62	−28.76	−25.60	−20.67	−12.57	−21.10	−22.00 ± 6.0[b]
	OR/EOPE	−23.74	−24.08	−26.05	−26.80	−23.94	−21.83	−17.88	−11.29	−19.00	
NH_3	SHG	−51.10	−51.90	−58.60	−61.82	−54.58	−51.37	−46.53	−21.97	−49.10	−48.40 ± 1.2[b]
	OR/EOPE	−35.03	−35.21	−38.02	−38.67	−36.71	−37.87	−35.72	−16.74	−38.30	
CO	SHG	27.99	26.82	29.35	26.01	25.85	26.73	25.55	24.10	27.00	29.90 ± 3.2[b]
	OR/EOPE	24.82	23.63	25.70	22.57	22.76	23.90	23.09	21.90	24.60	
HF	SHG	−11.09	−11.59	−12.69	−14.00	−12.09	−12.86	−10.35	−5.85	−8.00	−10.90 ± 1.0[c]
	OR/EOPE	−10.08	−10.52	−11.45	−12.61	−10.96	−11.74	−9.51	−5.52	−7.50	
H_2S	SHG	−6.74	−7.05	−6.95	−8.70	−8.21	−11.83	−10.06	2.38	−8.80	−9.95 ± 2.1[b]
	OR/EOPE	−5.11	−5.46	−4.81	−6.40	−6.40	−9.95	−8.83	2.12	−8.20	

[a]From Ref. 114.
[b]From Ref. 132.
[c]From Ref. 133.

is partially corrected by CAP-LYP. For CH_3F, for SHG, CAP-PBE gives a result very close to the MP2 hyperpolarizability augmented with TDHF dispersion.[121] However, these values underestimate (in absolute value) the experimental result.[122] On the other hand, CAP-LYP agrees very well with experiment, while all the other functionals yield overestimates (in absolute value). Nevertheless, in all cases, the sign of the hyperpolarizabilities is right, as also was presented in Table VI. For the SHG of CH_3CN, CAP-PBE is in a good agreement with respect to the CCSD(T) hyperpolarizability augmented with MP2 dispersion.[121] In general, all functionals and MP2 give overestimates relative to the experimental value.[123] In the case of CH_3Cl, for SHG, there is a sign inversion, with CAP-PBE giving one sign versus the rest of the functionals giving the other. However, the experimental reference[124] matches well with the CAP-PBE value. For SHG in CHF_3, all the functionals overestimate the absolute value compared to the corresponding experiment,[122] but once again CAP-PBE is closest to experiment.[122] In CF_3Cl, CAP-LYP and CAP-PBE SHG values are very close to experiment, unlike all the other

TABLE VII. Comparison of dynamic LDA and GGA TDADPT hyperpolarizabilities (in a.u.) of methane analogs with other theoretical and experimental results. The TDADPT values were calculated at the same wavelength as used in the corresponding experiments.

Molecule	Value	LDA	PBE	BLYP	OLYP	PBE-LS	CAP-LYP	CAP-PBE	Other theoretical results	Experimental
CH_3OH	SHG	−61.66	−62.23	−68.44	−73.86	−63.97	−54.37	−45.71	−40.61[a]	−35.0 ± 2.1[b]
	OR/EOPE	−51.39	−51.62	−56.02	−59.67	−53.00	−46.61	−39.63		
CH_3F	SHG	−70.81	−70.54	−76.79	−81.87	−69.64	−56.91	−48.56	−46.30[c]	−57.0 ± 4.2[d]
	OR/EOPE	−62.41	−61.96	−66.89	−70.78	−61.08	−51.17	−44.13	23.45[e]	
CH_3CN	SHG	25.20	24.75	24.32	23.86	22.42	29.81	27.51	27.48[f]	17.9 ± 1.1[g]
	OR/EOPE	24.08	23.69	23.29	22.93	21.53	28.59	26.92		
CH_3Cl	SHG	−4.13	−3.83	−7.40	−12.94	−2.02	−6.58	5.66		13.3 ± 1.4[h]
	OR/EOPE	−3.37	−3.13	−6.10	−10.73	−1.42	−4.96	5.57		
CHF_3	SHG	−36.86	−36.61	−38.79	−39.84	−36.49	−33.51	−32.95	−20.20[i]	−25.2 ± 0.9[j]
	OR/EOPE	−33.30	−32.97	−34.75	−35.54	−32.82	−30.79	−30.19	−19.40[k]	
CF_3Cl	SHG	−85.87	−86.93	−91.50	−89.71	−83.85	−78.46	−74.21		−69.2 ± 2.8[l]
	OR/EOPE	−76.73	−77.48	−81.28	−79.58	−74.66	−70.62	−67.12		
$CHCl_3$	SHG	−3.03	−3.70	−0.27	−6.29	−5.45	−13.43	−2.37		1.2 ± 2.6[m]
	OR/EOPE	−2.76	−3.35	−0.39	−5.59	−4.92	−11.48	−1.98		
$CFCl_3$	SHG	−37.24	−37.59	−38.41	−34.46	−34.30	−35.81	−31.88		−30.9 ± 9.6[n]
	OR/EOPE	−35.44	−35.67	−36.64	−33.27	−32.77	−33.93	−30.24		

[a]Dynamic value at λ = 694.3 nm, CCSD, from Ref. 115.
[b]Dynamic value at λ = 694.3 nm, electric field-induced second harmonic generation (ESHG), from Ref. 120.
[c]Dynamic value at λ = 632.8 nm, static β from MP2 with TDHF percentage dispersion from Ref. 121.
[d]Dynamic value at λ = 694.3 nm, ESHG, from Ref. 122.
[e]Dynamic value at λ = 694.3 nm, TDHF, from Ref. 117.
[f]Dynamic value at λ = 514.5 nm, static β from CCSD(T) with MP2 additive dispersion from Ref. 121.
[g]EFISH at λ = 1064 nm from Ref. 123.
[h]Dynamic value at λ = 694.3 nm, ESHG, from Ref. 124.
[i]Dynamic value at λ = 694.3 nm, TDHF, from Ref. 117.
[j]Dynamic value at λ = 694.3 nm, ESHG, from Ref. 122.
[k]Dynamic value at λ = 694.3 nm, TDHF, from Ref. 117.
[l]Dynamic value at λ = 694.3 nm, ESHG, from Ref. 122.
[m]Dynamic value at λ = 694.3 nm, ESHG, from Ref. 124.
[n]Dynamic value at λ = 694.3 nm, ESHG, from Ref. 124.

TABLE VIII. Comparison of the eigenvalues of the HOMO, LUMO, and immediately adjacent HOMO − 1, and LUMO + 1 in eV for the noble gas atoms as determined by exchange-only calculations with the universal gaussian basis set[a] for several X energy functionals.

Atom	Orbital	LDA	PBE	B88	OPTX	PBE-LS	CAP	HF
He	H	−14.067	−15.050	−15.078	−14.977	−15.234	−14.811	−24.979
	L	2.316	1.787	1.817	1.444	1.658	2.500	3.201
	L + 1	12.464	11.811	11.943	11.695	11.693	12.518	14.458
Ne	H − 1	−12.056	−12.395	−12.371	−12.369	−12.467	−12.151	−23.141
	H	−12.056	−12.395	−12.371	−12.369	−12.467	−12.151	−23.141
	L	3.241	2.714	2.807	2.409	2.576	3.514	4.173
	L + 1	3.241	2.714	2.807	2.409	2.576	3.514	4.173
Ar	H − 1	−9.081	−9.320	−9.298	−9.376	−9.369	−9.155	−16.082
	H	−9.081	−9.320	−9.298	−9.376	−9.369	−9.155	−16.082
	L	3.253	2.671	2.948	2.463	2.538	3.552	4.708
	L + 1	3.253	2.671	2.948	2.463	2.538	3.552	4.708
Kr	H − 1	−8.155	−8.316	−8.299	−8.384	−8.352	−8.181	−14.263
	H	−8.155	−8.316	−8.299	−8.384	−8.352	−8.181	−14.263
	L	1.400	0.917	1.216	1.038	0.812	1.664	3.528
	L + 1	3.366	2.809	3.115	2.690	2.687	3.651	5.028
Xe	H − 1	−7.215	−7.328	−7.315	−7.389	−7.354	−7.216	−12.439
	H	−7.215	−7.328	−7.315	−7.389	−7.354	−7.216	−12.439
	L	1.717	1.348	1.602	1.625	1.268	1.959	4.051
	L + 1	3.613	3.135	3.433	3.175	3.033	3.878	5.569
Rn	H − 1	−6.806	−6.896	−6.884	−6.948	−6.917	−6.786	−11.646
	H	−6.806	−6.896	−6.884	−6.948	−6.917	−6.786	−11.646
	L	0.349	−0.079	0.154	−0.110	−0.178	0.623	1.723
	L + 1	1.526	1.089	1.271	0.900	0.981	1.815	2.465

[a]Reference 93.

functionals. For $CHCl_3$, we find a large discrepancy between all functionals and the experimental reference for SHG.[124] However, we have not found theoretical results with which to compare. All DFT SHG values for $CFCl_3$ look similar, with CAP-PBE lying rather close to the experimental value.[124] In Table VII, one can also see OR and EOPE (electro-optical Pockels effect) values for the same systems, at the same wavelength of the SHG results. Unfortunately, in those cases, we have not found any reference results from highly correlated wavefunctions.

IV. POTENTIAL PROPERTIES

The CAP functional, Eq. (14) provides as good or better results on most of the standard sets as any other GGA and it does better on response properties than the others. Intriguingly, however, it does not lead to major changes in the eigenvalues for the highest occupied molecular orbitals (HOMOs) but does affect the lowest unoccupied molecular orbitals (LUMOs). Table VIII for the noble gas atoms and Table IX for some molecules illustrate the point with HOMO, LUMO, and imme-

TABLE IX. Comparison of the eigenvalues of the HOMO, LUMO, and immediately adjacent HOMO − 1, and LUMO + 1 in eV for several molecules.

Molecule	Orbital	LDA	PBE	BLYP	OLYP	PBE-LS	CAP-LYP	CAP-PBE
NH_3	H − 1	−11.353	−11.309	−11.238	−11.249	−11.331	−11.053	−11.097
	H	−6.204	−6.109	−6.038	−6.022	−6.117	−5.872	−5.908
	L	−0.479	−0.476	−0.634	−0.770	−0.552	0.503	0.920
	L + 1	2.332	2.346	2.161	2.000	2.261	3.056	3.510
C_6H_6	H − 1	−6.517	−6.318	−6.133	−6.152	−6.291	−5.959	−6.098
	H	−6.517	−6.318	−6.133	−6.152	−6.291	−5.957	−6.087
	L	−1.423	−1.208	−1.064	−1.039	−1.181	−0.835	−0.906
	L + 1	−1.423	−1.208	−1.064	−1.039	−1.181	−0.833	−0.901
CH_3OH	H − 1	−8.006	−7.962	−7.897	−7.921	−7.984	−7.676	−7.742
	H	−6.318	−6.221	−6.174	−6.155	−6.229	−5.962	−6.008
	L	−0.506	−0.479	−0.639	−0.773	−0.550	0.536	1.072
	L + 1	0.199	0.207	0.049	−0.076	0.139	1.363	1.785
CH_3CN	H − 1	−8.294	−8.123	−7.992	−8.000	−8.109	−7.782	−7.899
	H	−8.294	−8.123	−7.992	−7.997	−8.109	−7.769	−7.859
	L	−0.751	−0.746	−0.942	−1.064	−0.822	0.071	0.030
	L + 1	−0.468	−0.278	−0.210	−0.163	−0.267	0.076	0.095

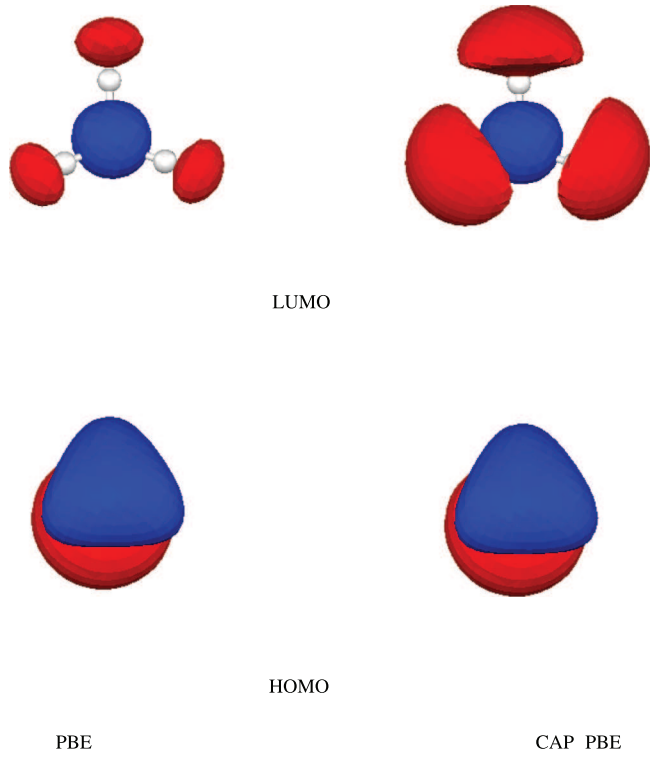

FIG. 6. Isosurface of the highest occupied and the lowest unoccupied molecular orbitals of NH_3 calculated with PBE (left) and CAP-PBE (right). The positive value of the isosurface is 0.05 (red), and the negative value is −0.05 (blue).

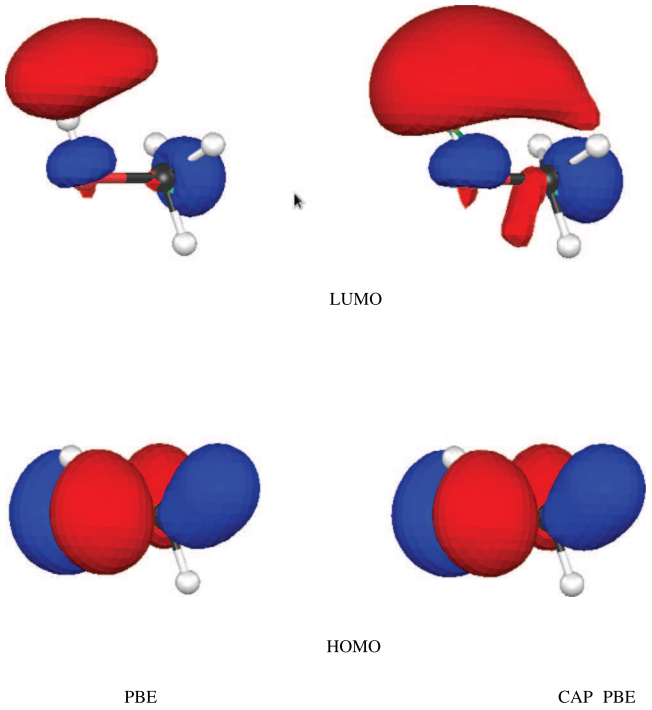

FIG. 7. Isosurface of the highest occupied and the lowest unoccupied molecular orbitals of CH_3OH calculated with PBE (left) and CAP-PBE (right). The positive value of the isosurface is 0.05 (red), and the negative value is −0.05 (blue).

diately adjacent ("HOMO − 1," "LUMO + 1") eigenvalues for several systems and XC functionals. Note that for the Rn atom and the NH_3, CH_3OH, and CH_3CN molecules, the CAP gives a positive energy LUMO, in contrast with the values from all the other functionals (Teale, De Proft, and Tozer[125] have reported such behavior for a potential with the correct asymptotic behavior). Such positive energy states cannot be bound states in a potential which vanishes as $-1/r$. Rather, they occur because of the confinement provided from the finite-sized L^2 basis set,[126] so detailed exploration is required, especially, in view of the good response property performance from CAP-PBE.

First, we observe that, in going from other functionals to CAP, the HOMOs and particularly the LUMOs do show slight to large changes in several cases. For example, Fig. 6 shows the slight shifts from PBE to CAP-PBE in the HOMO and LUMO of NH_3, while Fig. 7 shows the corresponding large changes in CH_3OH. These changes in the orbitals seem to be primarily responsible for the improvement observed in calculated response properties.

Obviously, the orbital changes among X functionals reflect differences in the potentials they generate. Keep in mind that CAP was constructed to fulfill constraints for $s \to 0$ and $r \to \infty$ and to provide a sensible, smooth connection between those limits. Fig. 8 provides comparison of v_x^{CAP} with other GGA X potentials and with the optimized effective potential (OEP), plot (a) corresponds to the domain $0 \le r \le 15$ a.u., and plot (b) corresponds to an amplification of the domain $1 \le r \le 15$ a.u. The OEP comes from the method of Talman and Shadwick[127] and values obtained by Engel and Vosko.[128] All the potentials

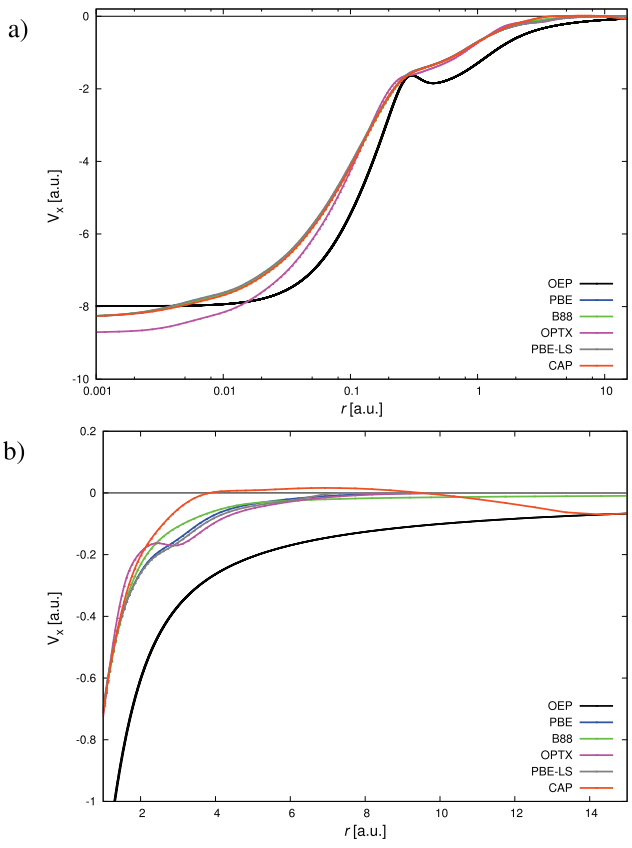

FIG. 8. (a) Plot of the exchange potential for Ne atom as a function of the distance in a. u., in the domain $0 \le r \le 15$, for several GGA approximations and for OEP. (b) Amplification of the same plot in the domain $1 \le r \le 15$.

in Fig. 8 correspond to exchange-only calculations. What one sees is that v_x^{CAP} has unexpected behavior. In particular, it very closely resembles a standard GGA potential in the HOMO energy range and below, but it is substantially higher than a standard GGA for larger r and even goes slightly positive. While that weakly positive region is unphysical, the combination has the pragmatically valuable consequence that the HOMO energy stays roughly fixed while the LUMO energy goes up, hence the LUMO orbital spreads out. This is not a direct consequence of the asymptotic condition but instead is an indirect result which occurs because of the interpolation between large and small s constraints.

That realization leads to a deeper insight. The Engel *et al.* constraint[76] given in Eq. (12) is not unique. It is a solution of the asymptotic differential equation for F_x^{GGA} (Eq. (11)), but not the only one possible. In particular, Gill and Pople[129] give the exact asymptotic behavior of the X enhancement function for atomic H as $s(\ln s)^{2/3}$. Thus, not only is Eq. (12) not unique but also it is inconsistent with at least one critical case. Imposition of the Gill-Pople asymptotic behavior would force a different interpolation to the $s \to 0$ limit, a topic we leave to future work. Similarly, we leave for the future the exploration of potentials which go to a constant because of the derivative discontinuity.[56,125,130]

V. CONCLUDING REMARKS

The analysis performed in Sec. III confirms that for thermodynamic, kinetic, and structural properties, the behavior of the enhancement function in the interval $0 \le s \le 3$ is crucial. Properties that depend on the response functions should depend upon the large s behavior associated with the functional derivative that leads to the X potential with the correct asymptotic behavior. But in practice, that behavior can be mimicked in the context of an L^2 basis set by a potential which goes high enough, exactly as v_x^{CAP} does.

The CAP X functional provides a description of properties that depend on total energy differences superior to or competitive with other GGA X functionals with the additional benefit of an improved description of properties that depend upon response functions as calculated via TDDFT in the ALDA. Based on the broad spectrum of quantities treated well by a single functional, we believe that the non-empirical CAP-PBE recommends itself as the best practical general purpose GGA XC functional presently available. We now are working to remove the mid-range positive behavior, to improve the correlation functional, and to add features related to the discontinuity of the exchange-correlation potential and the approximate satisfaction of the ionization-potential theorem.[131]

ACKNOWLEDGMENTS

We thank the Laboratorio de Supercómputo y Visualización of Universidad Autónoma Metropolitana-Iztapalapa for the use of their facilities. We also thank Eberhard Engel and Erin Johnson for providing us with OEP data for the Ne atom, and Jorge Garza for many useful discussions. J.C.-E. was supported in part by Conacyt through a postdoctoral fellowship. J.L.G. thanks Conacyt for Grant Nos. 128369 and 155698, and A.V. thanks Conacyt for Grant No. 128369. S.B.T. was supported in part by the U.S. Department of Energy Grant No. DE-SC-0002139.

APPENDIX: INGREDIENTS OF THE CAP POTENTIAL

For ease of programming, we provide explicit expressions for constructing v_x^{CAP}. From exact spin scaling, the spin-labeled exchange potential is

$$v_{x\sigma}^{GGA}[\rho_\sigma;\mathbf{r}] = \frac{\delta E_x^{GGA}[\rho_\uparrow,\rho_\downarrow]}{\delta\rho_\sigma(\mathbf{r})} = \left.\frac{\delta E_x^{GGA}[\rho]}{\delta\rho(\mathbf{r})}\right|_{\rho(\mathbf{r})=2\rho_\sigma(\mathbf{r})}, \tag{A1}$$

where $\sigma = \uparrow$ or $\downarrow$ and $\rho(\mathbf{r}) = \rho_\uparrow(\mathbf{r}) + \rho_\downarrow(\mathbf{r})$. With the CAP enhancement function, Eq. (14), the exchange potential is given by

$$\begin{aligned} v_{x\sigma}^{CAP}[\rho_\sigma;\mathbf{r}] = {} & A_x 2^{1/3}\rho_\sigma(\mathbf{r})^{1/3}\left[\frac{4}{3}F_x^{CAP}(s_\sigma)\right] \\ & + A_x 2^{1/3}\rho_\sigma(\mathbf{r})^{1/3}\left[-\frac{4}{3}s_\sigma(\mathbf{r}) - \frac{1}{2k_{F\sigma}}\frac{\nabla^2\rho_\sigma(\mathbf{r})}{|\nabla\rho_\sigma(\mathbf{r})|}\right. \\ & \left. + \frac{1}{2k_{F\sigma}}\frac{\nabla\rho_\sigma(\mathbf{r})\cdot\nabla|\nabla\rho_\sigma(\mathbf{r})|}{|\nabla\rho_\sigma(\mathbf{r})|^2}\right]\frac{dF_x^{CAP}(s_\sigma)}{ds_\sigma} \\ & + A_x 2^{1/3}\rho_\sigma(\mathbf{r})^{1/3} \\ & \times\left[-\frac{1}{(2k_{F\sigma})^2}\frac{\nabla\rho_\sigma(\mathbf{r})\cdot\nabla|\nabla\rho_\sigma(\mathbf{r})|}{|\nabla\rho_\sigma(\mathbf{r})|\rho_\sigma(\mathbf{r})} + \frac{4}{3}s_\sigma(\mathbf{r})^2\right] \\ & \times\frac{d^2F_x^{CAP}(s_\sigma)}{ds_\sigma{}^2}, \end{aligned} \tag{A2}$$

with $k_{F\sigma}(\mathbf{r}) = (6\pi^2\rho_\sigma(\mathbf{r}))^{1/3}$, $s_\sigma(\mathbf{r}) = \frac{1}{2k_{F\sigma}(\mathbf{r})}\frac{|\nabla\rho_\sigma(\mathbf{r})|}{\rho_\sigma(\mathbf{r})}$, $F_x^{CAP}(s_\sigma) = 1 - \frac{\alpha}{A_x}\frac{s_\sigma\ln(1+s_\sigma)}{1+c\ln(1+s_\sigma)}$, as in Eqs. (3) and (14), respectively. The required derivatives are

$$\frac{dF_x^{CAP}(s_\sigma)}{ds_\sigma} = -\frac{\alpha}{A_x}\frac{s_\sigma + (1+s_\sigma)\ln(1+s_\sigma)(1+c\ln(1+s_\sigma))}{(1+s_\sigma)(1+c\ln(1+s_\sigma))^2}, \tag{A3}$$

$$\frac{d^2F_x^{CAP}(s_\sigma)}{ds_\sigma{}^2} = -\frac{\alpha}{A_x}\frac{2+s_\sigma-2cs_\sigma+c(2+s_\sigma)\ln(1+s_\sigma)}{(1+s_\sigma)^2(1+c\ln(1+s_\sigma))^3}. \tag{A4}$$

[1]P. Hohenberg and W. Kohn, Phys. Rev. B **136**, B864 (1964).
[2]W. Kohn and L. J. Sham, Phys. Rev. **140**, 1133 (1965).
[3]R. G. Parr and W. T. Yang, *Density-Functional Theory of Atoms and Molecules* (Oxford University Press, New York, 1989).
[4]R. M. Dreizler and E. K. U. Gross, *Density Functional Theory* (Springer, Berlin, 1990).
[5]J. P. Perdew and S. Kurth, in *A Primer in Density Functional Theory*, edited by C. Fiolhais, F. Nogueira, and M. A. L. Marques (Springer, Berlin, 2003), p. 1.
[6]J. P. Perdew, A. Ruzsinszky, J. M. Tao, V. N. Staroverov, G. E. Scuseria, and G. I. Csonka, J. Chem. Phys. **123**, 062201 (2005).
[7]G. E. Scuseria and V. N. Staroverov, in *Theory and Applications of Computational Chemistry: The First Forty Years*, edited by C. Dykstra, G. Frenking, K. S. Kim, and G. E. Scuseria (Elsevier, Amsterdam, 2005), p. 669.
[8]E. Engel and R. M. Dreizler, *Density Functional Theory* (Springer-Verlag, Berlin, 2011).
[9]A. J. Cohen, P. Mori-Sanchez, and W. T. Yang, Chem. Rev. **112**, 289 (2012).
[10]K. Burke, J. Chem. Phys. **136**, 150901 (2012).
[11]A. D. Becke, J. Chem. Phys. **140**, 18A301 (2014).
[12]J. P. Perdew and K. Schmidt, in *Density Functional Theory and its Application to Materials*, edited by V. E. Van Doren, C. Van Alsenoy, and P. Geerlings (AIP, Melville, New York, 2001), p. 1.
[13]A. D. Becke, Phys. Rev. A **38**, 3098 (1988).
[14]C. T. Lee, W. T. Yang, and R. G. Parr, Phys. Rev. B **37**, 785 (1988).

[15]J. P. Perdew, K. Burke, and M. Ernzerhof, Phys. Rev. Lett. **77**, 3865 (1996); Erratum, **78**, 1396 (1997).
[16]N. C. Handy and A. J. Cohen, Mol. Phys. **99**, 403 (2001).
[17]L. A. Curtiss, K. Raghavachari, P. C. Redfern, and J. A. Pople, J. Chem. Phys. **112**, 7374 (2000).
[18]S. Parthiban and J. M. L. Martin, J. Chem. Phys. **114**, 6014 (2001).
[19]B. J. Lynch, Y. Zhao, and D. G. Truhlar, J. Phys. Chem. A **107**, 1384 (2003).
[20]V. N. Staroverov, G. E. Scuseria, J. M. Tao, and J. P. Perdew, J. Chem. Phys. **119**, 12129 (2003).
[21]Y. Zhao and D. G. Truhlar, J. Chem. Theory Comput. **1**, 415 (2005).
[22]Y. Zhao and D. G. Truhlar, J. Phys. Chem. A **109**, 5656 (2005).
[23]Y. Zhao, N. González-García, and D. G. Truhlar, J. Phys. Chem. A **109**, 2012 (2005).
[24]Y. Zhao, B. J. Lynch, and D. G. Truhlar, Phys. Chem. Chem. Phys. **7**, 43 (2005).
[25]Y. Zhao, N. E. Schultz, and D. G. Truhlar, J. Chem. Theory Comput. **2**, 364 (2006).
[26]Y. Zhao and D. G. Truhlar, J. Phys. Chem. A **110**, 10478 (2006).
[27]R. Peverati and D. G. Truhlar, "The quest for a universal density functional: The accuracy of density functionals across a broad spectrum of databases in chemistry and physics," e-print arXiv:1212.0944v4 [physics.chem-ph] (2013).
[28]P. R. Antoniewicz and L. Kleinman, Phys. Rev. B **31**, 6779 (1985).
[29]S. K. Ma and K. A. Brueckner, Phys. Rev. **165**, 18 (1968).
[30]L. A. Constantin, E. Fabiano, S. Laricchia, and F. D. Sala, Phys. Rev. Lett. **106**, 186406 (2011).
[31]J. M. del Campo, J. L. Gázquez, S. B. Trickey, and A. Vela, J. Chem. Phys. **136**, 104108 (2012).
[32]E. H. Lieb and S. Oxford, Int. J. Quantum Chem. **19**, 427 (1981).
[33]M. Levy and J. P. Perdew, Phys. Rev. B **48**, 11638 (1993); Erratum, **55**, 13321 (1997)
[34]A. Vela, V. Medel, and S. B. Trickey, J. Chem. Phys. **130**, 244103 (2009).
[35]J. P. Perdew, in *Electronic Structure of Solids '91*, edited by P. Ziesche and H. Eschrig (Akademie, Berlin, 1991), p. 11.
[36]A. Vela, J. C. Pacheco-Kato, J. L. Gázquez, J. M. del Campo, and S. B. Trickey, J. Chem. Phys. **136**, 144115 (2012).
[37]J. L. Gázquez, J. M. del Campo, S. B. Trickey, R. J. Alvarez-Mendez, and A. Vela, in *Concepts and Methods in Modern Theoretical Chemistry*, edited by S. K. Ghosh and P. K. Chattaraj (CRC Press, Boca Raton, 2013), p. 295.
[38]S. Kurth, J. Mol. Struct.: THEOCHEM **501**, 189 (2000).
[39]L. Pollack and J. P. Perdew, J. Phys.: Condens. Matter **12**, 1239 (2000).
[40]L. Chiodo, L. A. Constantin, E. Fabiano, and F. D. Sala, Phys. Rev. Lett. **108**, 126402 (2012).
[41]J. P. Perdew, A. Ruzsinszky, J. Sun, and K. Burke, J. Chem. Phys. **140**, 18A533 (2014).
[42]D. J. Lacks and R. G. Gordon, Phys. Rev. A **47**, 4681 (1993).
[43]R. van Leeuwen and E. J. Baerends, Phys. Rev. A **49**, 2421 (1994).
[44]J. P. Perdew and W. Yue, Phys. Rev. B **33**, 8800 (1986).
[45]E. D. Murray, K. Lee, and D. C. Langreth, J. Chem. Theory Comput. **5**, 2754 (2009).
[46]M. Petersilka, U. J. Gossmann, and E. K. U. Gross, Phys. Rev. Lett. **76**, 1212 (1996).
[47]M. E. Casida, in *Recent Developments and Applications in Density Functional Theory*, edited by J. M. Seminario (Elsevier, Amsterdam, 1996), p. 391.
[48]P. Bleiziffer, A. Hesselmann, C. J. Umrigar, and A. Görling, Phys. Rev. A **88**, 042513 (2013).
[49]J. P. Perdew and M. Levy, Phys. Rev. Lett. **51**, 1884 (1983).
[50]L. J. Sham and M. Schluter, Phys. Rev. Lett. **51**, 1888 (1983).
[51]J. P. Perdew, R. G. Parr, M. Levy, and J. L. Balduz, Phys. Rev. Lett. **49**, 1691 (1982).
[52]W. T. Yang, A. J. Cohen, and P. Mori-Sanchez, J. Chem. Phys. **136**, 204111 (2012).
[53]L. J. Sham, Phys. Rev. B **32**, 3876 (1985).
[54]C.-O. Almbladh and U. von Barth, Phys. Rev. B **31**, 3231 (1985).
[55]M. K. Harbola and V. Sahni, Phys. Rev. Lett. **62**, 489 (1989).
[56]D. J. Tozer and N. C. Handy, J. Chem. Phys. **109**, 10180 (1998).
[57]M. E. Casida and D. R. Salahub, J. Chem. Phys. **113**, 8918 (2000).
[58]M. Gruning, O. V. Gritsenko, S. J. A. van Gisbergen, and E. J. Baerends, J. Chem. Phys. **114**, 652 (2001).
[59]J. L. Gázquez, J. Garza, F. D. Hinojosa, and A. Vela, J. Chem. Phys. **126**, 214105 (2007).
[60]J. L. Gázquez, J. Garza, R. Vargas, and A. Vela, in *Recent Developments in Physical Chemistry*, edited by E. Diaz-Herrera and E. Juaristi (2008), Vol. 979, p. 11.
[61]A. Lembarki, F. Rogemond, and H. Chermette, Phys. Rev. A **52**, 3704 (1995).
[62]M. Gruning, O. V. Gritsenko, S. J. A. van Gisbergen, and E. J. Baerends, J. Chem. Phys. **116**, 9591 (2002).
[63]Q. Wu, P. W. Ayers, and W. T. Yang, J. Chem. Phys. **119**, 2978 (2003).
[64]A. Karolewski, R. Armiento, and S. Kummel, Phys. Rev. A **88**, 052519 (2013).
[65]M. Filatov and W. Thiel, Phys. Rev. A **57**, 189 (1998).
[66]P. Jemmer and P. J. Knowles, Phys. Rev. A **51**, 3571 (1995).
[67]E. Engel and S. H. Vosko, Phys. Rev. B **50**, 10498 (1994).
[68]J. Garza, J. A. Nichols, and D. A. Dixon, J. Chem. Phys. **112**, 7880 (2000).
[69]J. Garza, J. A. Nichols, and D. A. Dixon, J. Chem. Phys. **112**, 1150 (2000).
[70]N. Umezawa, Phys. Rev. A **74**, 032505 (2006).
[71]A. P. Gaiduk, D. Mizzi, and V. N. Staroverov, Phys. Rev. A **86**, 052518 (2012).
[72]A. P. Gaiduk, D. S. Firaha, and V. N. Staroverov, Phys. Rev. Lett. **108**, 253005 (2012).
[73]M. Hoffmann-Ostenhof and T. Hoffmann-Ostenhof, Phys. Rev. A **16**, 1782 (1977).
[74]Y. Tal, Phys. Rev. A **18**, 1781 (1978).
[75]M. Levy, J. P. Perdew, and V. Sahni, Phys. Rev. A **30**, 2745 (1984).
[76]E. Engel, J. A. Chevary, L. D. Macdonald, and S. H. Vosko, Z. Phys. D: At., Mol. Clusters **23**, 7 (1992).
[77]See supplementary material at http://dx.doi.org/10.1063/1.4906606 which contains the results for all the individual systems calculated in this work, and the detailed analysis of the Lieb-Oxford bound discussed in the article.
[78]A. Zupan, J. P. Perdew, K. Burke, and M. Causà, Int. J. Quantum Chem. **61**, 835 (1997).
[79]A. Zupan, K. Burke, M. Emzerhof, and J. P. Perdew, J. Chem. Phys. **106**, 10184 (1997).
[80]J. M. del Campo, J. L. Gázquez, R. J. Alvarez-Mendez, and A. Vela, Int. J. Quantum Chem. **112**, 3594 (2012).
[81]R. Armiento and S. Kummel, Phys. Rev. Lett. **111**, 036402 (2013).
[82]M. Valiev, E. J. Bylaska, N. Govind, K. Kowalski, T. P. Straatsma, H. J. J. Van Dam, D. Wang, J. Nieplocha, E. Apra, T. L. Windus, and W. de Jong, Comput. Phys. Commun. **181**, 1477 (2010).
[83]L. A. Curtiss, K. Raghavachari, P. C. Redfern, and J. A. Pople, J. Chem. Phys. **106**, 1063 (1997).
[84]F. Weigend and R. Ahlrichs, Phys. Chem. Chem. Phys. **7**, 3297 (2005).
[85]E. Fabiano, L. A. Constantin, and F. D. Sala, J. Chem. Theory Comput. **7**, 3548 (2011).
[86]P. A. M. Dirac, Math. Proc. Cambridge Philos. Soc. **26**, 376 (1930).
[87]S. H. Vosko, L. Wilk, and M. Nusair, Can. J. Phys. **58**, 1200 (1980).
[88]B. J. Lynch, Y. Zhao, and D. G. Truhlar, see http://t1.chem.umn.edu/db/ for the Minnesota databases for chemistry and solid state physics.
[89]L. A. Curtis, P. C. Redfern, and K. Raghavachari, Wiley Interdiscip. Rev.: Comput. Mol. Sci. **1**, 810 (2011).
[90]*CRC Handbook of Chemistry and Physics*, 83rd ed. (CRC, Boca Raton, FL, 2002).
[91]J. M. L. Martin, Chem. Phys. Lett. **303**, 399 (1999).
[92]K. P. Huber and G. Herzberg, *Molecular Spectra and Molecular Structure IV. Constants of Diatomic Molecules* (Van Nostrand, New York, 1979).
[93]E. V. R. de Castro and F. E. Jorge, J. Chem. Phys. **108**, 5225 (1998).
[94]S. V. Shedge, J. Carmona-Espíndola, S. Pal, and A. M. Köster, J. Phys. Chem. A **114**, 2357 (2010).
[95]J. Carmona-Espíndola, R. Flores-Moreno, and A. M. Köster, J. Chem. Phys. **133**, 084102 (2010).
[96]J. Carmona-Espíndola, R. Flores-Moreno, and A. M. Köster, Int. J. Quantum Chem. **112**, 3461 (2012).
[97]P. Calaminici, J. Carmona-Espíndola, G. Geudtner, and A. M. Köster, Int. J. Quantum Chem. **112**, 3252 (2012).
[98]S. V. Shedge, S. Pal, and A. M. Köster, Chem. Phys. Lett. **552**, 146 (2012).
[99]A. M. Köster, G. Geudtner, P. Calaminici, M. E. Casida, V. D. Dominguez-Soria, R. Flores-Moreno, G. U. Gamboa, A. Goursot, T. Heine, A. Ipatov, F. Janetzko, J. M. del Campo, J. U. Reveles, A. Vela, B. Zuñiga-Gutierrez, and D. R. Salahub, deMon2k, version 3, The deMon Developers, Cinvestav, México, 2011.
[100]G. Geudtner, P. Calaminici, J. Carmona-Espíndola, J. M. del Campo, V. D. Dominguez-Soria, R. Flores-Moreno, G. U. Gamboa, A. Goursot, A. M. Köster, J. U. Reveles, T. Mineva, J. M. Vasquez-Perez, A. Vela, B. Zuñiga-Gutierrez, and D. R. Salahub, Wiley Interdiscip. Rev.: Comput. Mol. Sci. **2**, 548 (2012).
[101]P. Calaminici, K. Jug, and A. M. Köster, J. Chem. Phys. **109**, 7756 (1998).

[102]P. Calaminici, K. Jug, A. M. Köster, V. E. Ingamells, and M. G. Papadopoulos, J. Chem. Phys. **112**, 6301 (2000).
[103]J. C. Boettger and S. B. Trickey, Phys. Rev. B **53**, 3007 (1996).
[104]A. M. Köster, J. Chem. Phys. **118**, 9943 (2003).
[105]P. Calaminici, F. Janetzko, A. M. Köster, R. Mejia-Olvera, and B. Zuniga-Gutierrez, J. Chem. Phys. **126**, 044108 (2007).
[106]S. J. A. van Gisbergen, J. G. Snijders, and E. J. Baerends, J. Chem. Phys. **109**, 10657 (1998).
[107]M. Stener, G. Fronzoni, and M. de Simone, Chem. Phys. Lett. **373**, 115 (2003).
[108]M. Seth, G. Mazur, and T. Ziegler, Theor. Chem. Acc. **129**, 331 (2011).
[109]A. M. Köster, R. Flores-Moreno, and J. U. Reveles, J. Chem. Phys. **121**, 681 (2004).
[110]G. Herzberg, *Electronic Spectra and Electronic Structure of Polyatomic Molecules* (Van Nostrand Reinhold Company, New York, 1966).
[111]J. H. Callomon, E. Hirota, K. Kuchitsu, W. J. Lafferty, A. G. Maki, and C. S. Pote, *Landolt-Bornstein: Group II, Atomic and Molecular Physics*, Volume 7, Structure Data of Free Polyatomic Molecules (Springer-Verlag, Berlin, 1976).
[112]K. Kuchitsu, *Landolt-Bornstein: Group II Molecules and Radicals*, Volume 25, Structure Data of Free Polyatomic Molecules (Springer-Verlag, Berlin, 1999).
[113]M. W. Chase, C. A. Davies, J. R. Downey, D. J. Frurip, R. A. McDonald, and A. N. Syverud, in *JANAF Thermochemical Tables*, 3rd ed., Suppl. 1 from J. Phys. Chem. Ref. Data, Vol. 14 (AIP, 1985).
[114]H. Sekino and R. J. Bartlett, J. Chem. Phys. **98**, 3022 (1993).
[115]A. S. Dutra, M. A. Castro, T. L. Fonseca, E. E. Fileti, and S. Canuto, J. Chem. Phys. **132**, 034307 (2010).
[116]A. M. Lee and S. M. Colwell, J. Chem. Phys. **101**, 9704 (1994).
[117]H. Sekino and R. J. Bartlett, J. Chem. Phys. **85**, 976 (1986).
[118]G. U. Gamboa, P. Calaminici, G. Geudtner, and A. M. Köster, J. Phys. Chem. A **112**, 11969 (2008).
[119]G. R. Alms, A. K. Burnham, and W. H. Flygare, J. Chem. Phys. **63**, 3321 (1975).
[120]G. Maroulis, Chem. Phys. Lett. **195**, 85 (1992).
[121]D. P. Shelton and J. E. Rice, Chem. Rev. **94**, 3 (1994).
[122]J. F. Ward and I. J. Bigio, Phys. Rev. A **11**, 60 (1975).
[123]P. Kaatz, E. A. Donley, and D. P. Shelton, J. Chem. Phys. **108**, 849 (1998).
[124]C. K. Miller and J. F. Ward, Phys. Rev. A **16**, 1179 (1977).
[125]A. M. Teale, F. De Proft, and D. J. Tozer, J. Chem. Phys. **129**, 044110 (2008).
[126]N. Rösch and S. B. Trickey, J. Chem. Phys. **106**, 8940 (1997).
[127]J. D. Talman and W. F. Shadwick, Phys. Rev. A **14**, 36 (1976).
[128]E. Engel and S. H. Vosko, Phys. Rev. A **47**, 2800 (1993).
[129]P. M. W. Gill and J. A. Pople, Phys. Rev. A **47**, 2383 (1993).
[130]D. J. Tozer, Phys. Rev. A **56**, 2726 (1997).
[131]J. P. Perdew and M. Levy, Phys. Rev. B **56**, 16021 (1997).
[132]J. F. Ward and C. K. Miller, Phys. Rev. A **19**, 826 (1979).
[133]J. W. Dudley and J. F. Ward, J. Chem. Phys. **82**, 4673 (1985).